

Observational Study of Higher Dimensional Magnetic Universe in Non-linear Electrodynamics

Chayan Ranjit¹

Shuvendu Chakraborty²

Ujjal Debnath³

December 25, 2017

Received _____; accepted _____

arXiv:1304.1281v1 [physics.gen-ph] 4 Apr 2013

¹Department of Mathematics, Seacom Engineering College, Howrah - 711 302, India. Email: chayanranjit@gmail.com

²Department of Mathematics, Seacom Engineering College, Howrah - 711 302, India. Email:shuvendu.chakraborty@gmail.com

³Department of Mathematics, Bengal Engineering and Science University, Shibpur, Howrah-711 103, India. Email: ujjaldebnath@yahoo.com

ABSTRACT

In this work, we have considered the flat FRW model of the universe in $(n + 2)$ -dimensions filled with the dark matter and the magnetic field. We present the Hubble parameter in terms of the observable parameters Ω_{m0} and H_0 with the redshift z and the other parameters like $B_0, \omega, \mu_0, \delta, n, w_m$. The natures of magnetic field B , deceleration parameter q and Om diagnostic have also been analyzed for accelerating expansion of the universe. From Stern data set (12 points), we have obtained the bounds of the arbitrary parameters by minimizing the χ^2 test. The best-fit values of the parameters are obtained by 66%, 90% and 99% confidence levels. Now to find the bounds of the parameters (B_0, ω) and to draw the statistical confidence contour, we fixed four parameters μ_0, δ, n, w_m . Here the parameter n determines the higher dimensions and we perform comparative study between three cases : 4D ($n = 2$), 5D ($n = 3$) and 6D ($n = 4$) respectively. Next due to joint analysis with BAO observation, we have also obtained the bounds of the parameters (B_0, ω) by fixing other parameters μ_0, δ, n, w_m for 4D, 5D and 6D. The best fit of distance modulus for our theoretical model and the Supernova Type Ia Union2 sample are drawn for different dimensions.

Subject headings: Higher Dimension; Om Diagnostic; Observational Data; Observational Constraints.

1. Introduction

The origin of the classical Einstein field equations are Maxwell's electrodynamics which leads to the singular isotropic Friedmann solutions. Over the last few years the standard cosmological model, based on Friedmann-Robertson-Walker (FRW) geometry with Maxwell's electrodynamics has got sufficient amount of interest and many significant result are obtained ?Murphy (1973); De Sitter (1917); Novello et al (1979, 1993); Breton et al (2005, 2000); Novello (2005); Klippert et al (2000). Recently the non-linear electrodynamics (NLED) is a very interesting subject of research in general relativity. In 1934, Born and Infeld Bron et al (1934) wanted to modify the standard Maxwell theory in order to eliminate the problem of infinite energy of electron. In present time a new approach De Lorenci et al (2002) has been taken to avoid the cosmic singularity through a nonlinear extension of the Maxwell's electromagnetic theory and black hole solution can be obtained Kats et al (2007); Anninos et al (2009); Cai et al (2008). Another interesting feature can be viewed that for construction of regular black hole solutions Beato et al (1998, 1999); Salazar et al (1987), nonlinear electrodynamics theories are most powerful tool. The solution of the Einstein field equations together with NLED signifies the nonlinear effects in strong gravitational and magnetic fields. In the standard Maxwell Lagrangian, the nonlinear terms can be added by imposing the existence of symmetries such as parity conservation, gauge invariance, Lorentz invariance, etc. Novello et al (1996); Munoz (1996), as well as by the introduction of first order quantum corrections invariance to the Maxwell electrodynamics Heisenberg et al (1936); Schwinger (1951).

Our theoretical models are continuously testing by the different observational data. Currently the universe is expanding with acceleration which is verified by different observations of the SNeIa Perlmutter et al (1998, 1999); Riess et al (1998, 2004), large scale redshift surveys Bachall et al (1999); Tedmark et al (2004), the measurements of the cosmic microwave background (CMB) Miller et al (1999); Bennet et al (2000) and WMAP Briddle et al (2003); Spergel et al (2003). The observational facts are not clearly described by the standard big

bang cosmology with perfect fluid. Recently several interesting mechanisms such as loop quantum cosmology Asthekar et al (2011), modified gravity Cognola et al (2009), higher dimensional phenomena Chakraborty et al (2010); Ranjit et al (2012), Brans-Dicke theory Brans et al (1961), brane-world model Gergely et al (2002) and so on, suggested that some unknown matters are responsible for accelerating scenario of the universe which has positive energy density and sufficient negative pressure, known as dark energy Sahni et al (2000); Padmanabhan (2003). The most suitable type of dark energy for that scenario is the scalar field or quintessence Peebles et al (1988) in which the potential dominates over the kinetic term. In the present time several cosmological models have been constructed by introducing dark energies such as phantom Caldwell (2002); Bronnikov et al (2012); Chang et al (2012), tachyon scalar field Sen (2002); Balart et al (2007); Farajollahi et al (2011); Del Campo et al (2009), hessence Wei et al (2005), dilaton scalar field Morris (2012); Marcus (1990), K-essence scalar field Armendariz-Picon et al (2001); Bouhmadi et al (2010); Malquarti et al (2003), DBI essence scalar field Spalinski (2007); Martin et al (2008) and many others. Recent observational evidence suggests that the present Universe is formed of $\sim 26\%$ matter (baryonic + dark matter) and $\sim 74\%$ of a smooth vacuum energy component and about 0.01% of the thermal CMB component. The information about the structure formation process and other important cosmic observable are obtained by the angular power spectrum of CMB components in anisotropic.

Brief review of Maxwell's electrodynamics and non-linear electrodynamics are presented in section II. The basic equations in $(n + 2)$ -dimensional FRW universe and their solutions are given in section III for interacting model. The nature of Om-diagnostic are studied also. The observational data analysis mechanism for non-linear electrodynamic are described in section IV. The χ_{min}^2 test for best fit values of the observational parameters are investigated with Stern and then Stern+BAO joint data analysis. The best fit of distance modulus for our theoretical model and the Supernova Type Ia Union2 sample are drawn for different dimensions. Finally, some observational conclusions are drawn in section V.

2. Non-linear Electrodynamics

The Lagrangian density in Maxwell's electrodynamics can be written as Camara et al (2004)

$$\mathcal{L}_{(MAXWELL)} = -\frac{1}{4\mu_0} F^{\mu\nu} F_{\mu\nu} = -\frac{1}{4\mu_0} F \quad (1)$$

where $F^{\mu\nu}$ is the electromagnetic field strength tensor, F is the electromagnetic field and μ_0 is the magnetic permeability. The canonical energy-momentum tensor is then given by

$$T_{\mu\nu}^{(MAXWELL)} = \frac{1}{\mu_0} \left(F_{\mu\alpha} F_{\nu}^{\alpha} + \frac{1}{4} F g_{\mu\nu} \right) \quad (2)$$

The general class of Lagrangian for non-linear electromagnetic field Novello et al (2004) can be written in the form

$$\mathcal{L} = \sum_k c_k F^k \quad (3)$$

where the sum may involve both positive and negative powers of k .

Here we consider the generalization of Maxwell's electro-magnetic Lagrangian up to the second order terms of the fields as in the form Camara et al (2004)

$$\mathcal{L} = -\frac{1}{4\mu_0} F + \omega F^2 + \eta F^{*2} \quad (4)$$

where, ω and η are arbitrary constants. Here

$$F^{*2} \equiv F_{\mu\nu}^* F^{\mu\nu} \quad (5)$$

where, $F_{\mu\nu}^*$ is the dual of $F_{\mu\nu}$. Now, the electro-magnetic field F has the expression

in terms of electric field E and magnetic field B as in the form $F = 2(B^2 - E^2)$. So the corresponding energy-momentum tensor for non-linear electro-magnetic theory has the form

$$T_{\mu\nu} = -4 \frac{\partial \mathcal{L}}{\partial F} F_{\mu}^{\alpha} F_{\alpha\nu} + \left(\frac{\partial \mathcal{L}}{\partial F^*} F^* - \mathcal{L} \right) g_{\mu\nu} \quad (6)$$

Now we consider the homogeneous electric field E in plasma gives rise to an electric current of charged particles and then rapidly decays. So the squared magnetic field B^2 dominates over E^2 , i.e., in this case, $F = 2B^2$. So F is now only the function of magnetic field (vanishing electric component) and hence the FRW universe may be called *Magnetic Universe*. Now from equation (6), we obtain the expressions of magnetic density and pressure as

$$\rho_B = \frac{B^2}{2\mu_0} (1 - 8\mu_0\omega B^2) \quad (7)$$

and

$$p_B = \frac{1}{6\mu_0} B^2 (1 - 40\mu_0\omega B^2) = \frac{1}{3} \rho_B - \frac{16}{3} \omega B^4 \quad (8)$$

It is to be noted that the density ρ_B of the magnetic field must be positive, so the magnetic field B must satisfy $B < \frac{1}{2\sqrt{2\mu_0\omega}}$ with $\mu_0 > 0$ and $\omega > 0$. If $\frac{1}{2\sqrt{6\mu_0\omega}} < B < \frac{1}{2\sqrt{2\mu_0\omega}}$, the strong energy condition is violated i.e., $\rho_B + 3p_B = \frac{B^2}{\mu_0} (1 - 24\mu_0\omega B^2) < 0$ and in this case, the magnetic field generates dark energy which drives acceleration of the universe.

3. Field Equations and Solutions of Higher Dimensional FRW Model

We consider the $(n + 2)$ -dimensional flat homogeneous and isotropic universe described by FRW metric which is given by Chatterjee; Mukhopadhyay et al

$$ds^2 = -dt^2 + a^2(t)[dr^2 + r^2 dx_n^2] \quad (9)$$

where $a(t)$ is the scale factor and

$$dx_n^2 = d\theta^2 + \sin^2\theta_1 d\theta_2^2 + \dots + \sin^2\theta_1 \sin^2\theta_2 \dots \sin^2\theta_{n-1} d\theta_n^2 \quad (10)$$

Now assume that the universe is filled with dark matter and magnetic field type dark energy, so the Einstein's field equations in higher dimension are given by

$$\frac{n(n+1)}{2} \left(\frac{\dot{a}}{a}\right)^2 = \rho_{total} \quad (11)$$

and

$$n\frac{\ddot{a}}{a} + \frac{n(n-1)}{2} \left(\frac{\dot{a}}{a}\right)^2 = -p_{total} \quad (12)$$

where

$$\rho_{total} = \rho_m + \rho_B = \rho_m + \frac{B^2}{2\mu_0}(1 - 8\mu_0\omega B^2) \quad (13)$$

and

$$p_{total} = p_m + p_B = w_m\rho_m + \left(\frac{1}{3}\rho_B - \frac{16}{3}\omega B^4\right) \quad (14)$$

where $8\pi G = c = 1$. Also ρ_m and p_m are the energy density and pressure of the dark matter with the equation of state given by $p_m = w_m\rho_m$, $-1 \leq w_m \leq 1$ and ρ_B and p_B are the energy density and pressure due to magnetic field. The energy conservation equation in higher dimensional cosmology is given by

$$\dot{\rho}_{total} + (n+1)H(\rho_{total} + p_{total}) = 0 \quad (15)$$

where H is the Hubble parameter defined as $H = \frac{\dot{a}}{a}$. According to the recent Supernovae and CMB data, the energy transfer decay rate should be proportional to the present value of the Hubble parameter. Then we consider the model of interaction between dark matter and dark energy governed by the magnetic field, through a phenomenological interaction term Q .

Hence the energy-conservation equation (15) becomes

$$\dot{\rho}_m + (n+1)H(\rho_m + p_m) = +Q \quad (16)$$

and

$$\dot{\rho}_B + (n+1)H(\rho_B + p_B) = -Q \quad (17)$$

For simplicity of the calculation, we take the interaction component as Bandyopadhyay et al (2011)

$$Q = (n+1)\delta \frac{B}{\mu_0} (1 - 16\mu_0\omega B^2)H \quad (18)$$

where, δ is a small positive quantity, termed as interaction parameter. Using the above expressions of ρ_B , p_B and solving the equations (16)-(18) we obtain Bandyopadhyay et al (2011)

$$B = -\frac{3}{2}\delta + \frac{B_0 + \frac{3\delta}{2}}{(1+z)^{-\frac{2}{3}(n+1)}}, \quad B_0 \text{ being a constant.} \quad (19)$$

and

$$\begin{aligned} \rho_m = & \frac{\rho_{m0}}{(1+z)^{-(n+1)(w_m+1)}} + \frac{\delta}{2\mu_0(1+z)^{-(n+1)(w_m+1)}} \left[\frac{32\omega\mu_0(B_0 + \frac{3\delta}{2})^3}{w_m - 1} (1 - (1+z)^{-(n+1)(w_m-1)}) \right. \\ & - \frac{3\delta(-1 + 36\delta^2\omega\mu_0)}{w_m + 1} (1 - (1+z)^{-(n+1)(w_m+1)}) - \frac{432\delta\omega\mu_0(B_0 + \frac{3\delta}{2})^2}{3w_m - 1} (1 - (1+z)^{-\frac{1}{3}(n+1)(3w_m-1)}) \\ & \left. + \frac{6(B_0 + \frac{3\delta}{2})(-1 + 108\delta^2\omega\mu_0)}{3w_m + 1} (1 - (1+z)^{-\frac{1}{3}(n+1)(3w_m+1)}) \right] \quad (20) \end{aligned}$$

where ρ_{m0} is a constant and redshift $z = \frac{1}{a} - 1$. From the above solutions, it may be concluded that the interaction term Q always decays with the evolution of the universe. If

$\delta = 0$, we get the non-interacting solutions, i.e., $B \propto a^{-2\frac{(n+1)}{3}}$. When $n = 2$ (i.e., for 4D), we can recover the result of Ref Bandyopadhyay et al (2011) (i.e., $B \propto a^{-2}$) and also when $\delta = 0$, $n = 2$ and we drop the matter density term (i.e., $\rho_m = 0$), then we can verify the result of Ref. Camara et al (2004) for $\Lambda = 0$. Otherwise, our solutions are not similar with their solutions.

The Hubble parameter and **Deceleration parameter** are given by

$$H^2(z) = \frac{2\rho_m + \frac{B^2}{\mu_0}(1 - 8\mu_0\omega B^2)}{n(n+1)} \quad (21)$$

and

$$q = -1 - \frac{\dot{H}}{H^2} = \frac{n-1}{2} + \frac{n+1}{6} \left[\frac{3w_m\rho_m - 16\omega B^4 + \frac{B^2}{2\mu_0}(1 - 8\mu_0\omega B^2)}{\rho_m + \frac{B^2}{2\mu_0}(1 - 8\mu_0\omega B^2)} \right] \quad (22)$$

where B and ρ_m are given by (19) and (20). The expression of q is very complicated in terms of z . So the variation of deceleration parameter q against redshift z is plotted in figure 1 for 4D ($n = 2$), 5D ($n = 3$) and 6D ($n = 3$). From figure, we see that q decreases from some positive value to -1 as z decreases. So the model generates first deceleration and then acceleration as universe expands.

• **Om DIAGNOSTIC:**

Recently, Sahni et al Sahni et al (2003, 2008) proposed a new cosmological parameter named Om which is a combination of Hubble parameter and the cosmological redshift and provides a null test of dark energy. Om diagnostic has been discussed together with statefinder for generalized Chaplygin gas model from cosmic observations in Tong et al (2009); Lu et al (2009). Generally, it was introduced to differentiate Λ CDM from other dark energy models. For Λ CDM model, $Om = \Omega_{m0}$ is a constant, independent of redshift z . Also it helps to distinguish the present matter density constant Ω_{m0} in different models more effectively. The main utility for Om diagnostic is that the quantity of Om can distinguish dark energy models

with less dependence on matter density Ω_{m0} relative to the EoS of dark energy. Our starting point for Om diagnostics in the Hubble parameter and it is defined as:

$$Om(z) = \frac{h^2(x) - 1}{x^3 - 1} \quad (23)$$

where $x = z + 1$ and $h(x) = \frac{H(x)}{H_0} \equiv \tilde{H}$ and H_0 is the present value of the Hubble parameter. Now in our interacting magnetic field model, we obtain

$$Om(z) = \frac{\tilde{H}^2(z) - 1}{(1+z)^3 - 1} = \frac{\frac{2\rho_m + \frac{B^2}{\mu_0}(1-8\mu_0\omega B^2)}{n(n+1)H_0^2} - 1}{(1+z)^3 - 1} \quad (24)$$

where $\tilde{H}^2(z) = \frac{H^2(z)}{H_0^2}$. We draw the Om diagnostic against redshift z in figure 2 for 4D, 5D and 6D. The Om diagnostic always increases as z decreases (universe expands).

4. Observational Constraints

In this section, we investigate the observational constraints of the higher dimensional FRW model of the magnetic universe. We shall determine the expected bounds of the theoretical parameters by χ^2 statistical best fit test with the basis of $H(z)$ - z (Stern) Stern et al (2010) and Stern+BAO Wu et al (2007); Thakur et al (2009); Paul et al; Paul et al; Ghose et al; Chakraborty et al (2012) joint data analysis. We also determine the statistical confidence contours between two parameters ω and B_0 in different dimensions. The best fit of distance modulus for our theoretical model and the Supernova Type Ia Union2 sample are analyzed for different dimensions. To investigate the bounds of model parameters here we consider Stern ($H(z)$ - z) data set with 12 data of $H(z)$ - z (Stern) in the following Table 1 Stern et al (2010).

z	$H(z)$	$\sigma(z)$
0	73	± 8
0.1	69	± 12
0.17	83	± 8
0.27	77	± 14
0.4	95	± 17.4
0.48	90	± 60
0.88	97	± 40.4
0.9	117	± 23
1.3	168	± 17.4
1.43	177	± 18.2
1.53	140	± 14
1.75	202	± 40.4

Table 1: $H(z)$ and $\sigma(z)$ for different values of z .

Defining $\Omega_{m0} = \frac{\rho_{m0}}{\frac{n(n+1)}{2}H_0^2}$ and using the expression of ρ_m and B , the expression of $H^2(z)$ becomes

$$H^2(z) = \frac{H_0^2 \Omega_{m0}}{(1+z)^{-(n+1)(w_m+1)}} + \frac{\delta}{n(n+1)\mu_0(1+z)^{-(n+1)(w_m+1)}} \left[\frac{32\omega\mu_0(B_0 + \frac{3\delta}{2})^3}{w_m - 1} (1 - (1+z)^{-(n+1)(w_m-1)}) \right. \\ \left. - \frac{3\delta(-1 + 36\delta^2\omega\mu_0)}{w_m + 1} (1 - (1+z)^{-(n+1)(w_m+1)}) - \frac{432\delta\omega\mu_0(B_0 + \frac{3\delta}{2})^2}{3w_m - 1} (1 - (1+z)^{-\frac{1}{3}(n+1)(3w_m-1)}) \right]$$

$$\begin{aligned}
& + \frac{6(B_0 + \frac{3\delta}{2})(-1 + 108\delta^2\omega\mu_0)}{3w_m + 1} \left(1 - (1+z)^{-\frac{1}{3}(n+1)(3w_m+1)} \right) \Big] \\
& + \frac{\left(-\frac{3}{2}\delta + \frac{B_0 + \frac{3\delta}{2}}{(1+z)^{-\frac{2}{3}(n+1)}} \right)^2}{n(n+1)\mu_0} \left[1 - 8\mu_0\omega \left(-\frac{3}{2}\delta + \frac{B_0 + \frac{3\delta}{2}}{(1+z)^{-\frac{2}{3}(n+1)}} \right)^2 \right] \quad (25)
\end{aligned}$$

This equation can be written in the form $H(z) = H_0E(z)$, where $E(z)$ known as normalized Hubble parameter contains six model parameters $\mu_0, B_0, \omega, \delta, n, w_m$ beside the redshift parameter z . Now to find the bounds of the parameters and to draw the statistical confidence contour (66%, 90% and 99% confidence levels) we fixed four parameters μ_0, n, δ, w_m . In the this case we find the bounds of B_0, ω and draw the contours between them. Here the parameter n determines the higher dimensions and we perform comparative study between three cases : 4D ($n = 2$), 5D ($n = 3$) and 6D ($n = 4$) respectively.

4.1. Analysis with Stern ($H(z)$ - z) Data Set

Here we analyze the model parameters using twelve data Stern et al (2010) of Hubble parameter for different redshift given by Table 1. We first form the Chi square statistic (with 11 degree of freedom) as a sum of standard normal distribution as follows:

$$\chi_O^2 = \sum \frac{(H_E(H_0, B_0, \mu_0, n, w_m, \omega, \delta, , z) - H_{OB})^2}{2\sigma^2} \quad (26)$$

where H_E and H_{OB} are theoretical and observed values of Hubble parameter at different redshifts respectively and σ is the corresponding error. Here, H_0 is a nuisance parameter and can be safely marginalized. We consider the observed parameters $\Omega_{m0} = 0.28$, $H_0 = 72 \pm 8$ Kms⁻¹ Mpc⁻¹ and a fixed prior distribution. Here we shall determine the model parameters B_0, ω by minimizing the χ^2 statistic. The reduced chi square can be written as

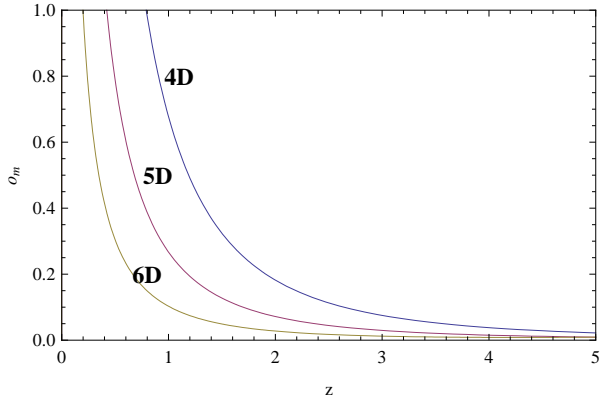


Fig.1

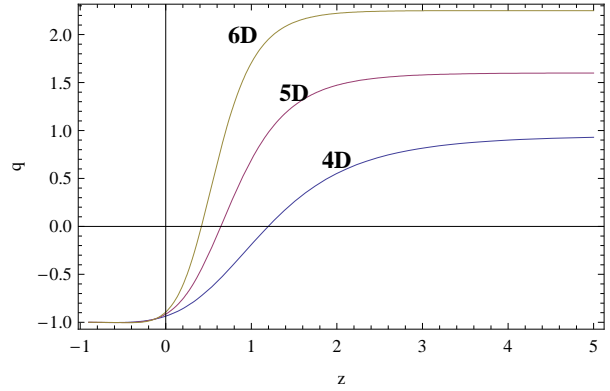


Fig.2

Figs. 1 and 2 represent the variations of deceleration parameter q and Om diagnostic against redshift z respectively for 4D, 5D and 6D.

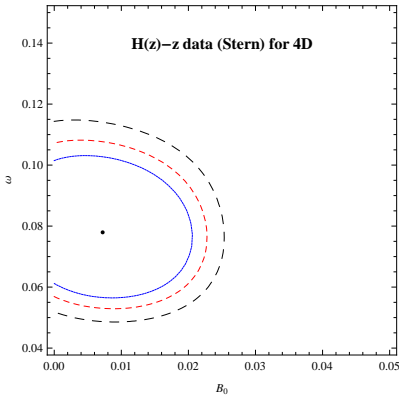


Fig.3

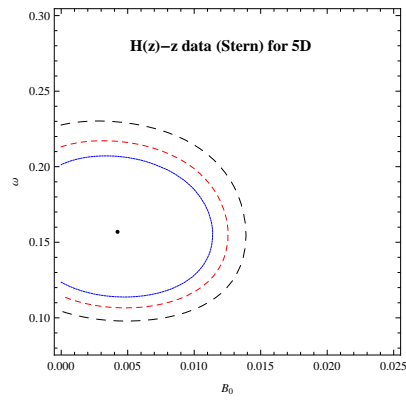


Fig.4

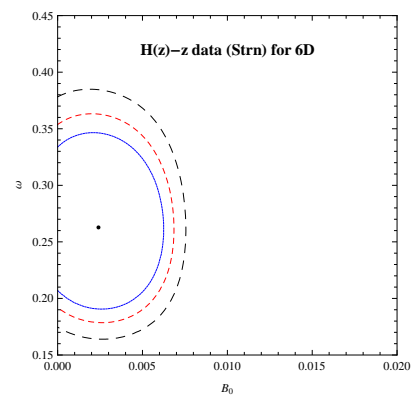


Fig.5

Figs. 3 - 5 show that the variations of ω against B_0 in 4D, 5D and 6D respectively for different confidence levels. The 66% (solid, blue), 90% (dashed, red) and 99% (dashed, black) contours are plotted in these figures for the $H(z)$ - z (Stern) analysis.

$$\chi_R^2 = -2 \ln \int \left[e^{-\frac{\chi^2}{2}} P(H_0) \right] dH_0 \quad (27)$$

where $P(H_0)$ is the prior distribution. We now plot the graphs for different confidence levels (i.e., 66%, 90% and 99% confidence levels) and for three different dimensions (4D, 5D and 6D). Now our best fit analysis with Stern observational data support the theoretical range of the parameters. When we fix the parameters $\mu_0 = 0.7, \delta = 0.01, w_m = 0.1$, the 66% (solid, blue), 90% (dashed, red) and 99% (dashed, black) contours for (B_0, ω) are plotted in figures 3, 4 and 5 for 4D ($n = 2$), 5D ($n = 3$) and 6D ($n = 4$) respectively. The best fit values of (B_0, ω) and minimum values of χ^2 for different values of $n = 2, 3, 4$ (i.e., different dimensions) are tabulated in Table 2. For each dimension, we compare the model parameters through the values of the parameters and by the statistical contours. From this comparative study, one can understand the convergence of theoretical values of the parameters to the values of the parameters obtained from the observational data set and how it changes from normal four dimension to higher dimension (6D).

n	B_0	ω	χ_{min}^2
2(4D)	0.007	0.078	68.796
3(5D)	0.004	0.157	68.150
4(6D)	0.002	0.263	67.694

Table 2: $H(z)$ - z (Stern): The best fit values of B_0 , ω and the minimum values of χ^2 for different dimensions.

4.2. Joint Analysis with Stern + BAO Data Sets

The Baryon Acoustic Oscillations (BAO) in the primordial baryon-photon fluid, leave a characteristic signal on the galaxy correlation function, a bump at a scale ~ 100 Mpc, as observed by Eisenstein et al Eisenstein et al (2005). We shall investigate the two parameters

B_0 and ω for our model using the BAO peak joint analysis for low redshift (with range $0 < z < 0.35$) using standard χ^2 distribution. The BAO peak parameter may be defined by

$$\mathcal{A} = \frac{\sqrt{\Omega_m}}{E(z_1)^{1/3}} \left(\frac{1}{z_1} \int_0^{z_1} \frac{dz}{E(z)} \right)^{2/3} \quad (28)$$

where

$$\Omega_m = \Omega_{m0}(1 + z_1)^3 E(z_1)^{-2} \quad (29)$$

Here, $E(z)$ is the normalized Hubble parameter and $z_1 = 0.35$ is the typical redshift of the SDSS data sample. This quantity can be used even for more general models which do not present a large contribution of dark energy at early times. Now the χ^2 function for the BAO measurement can be written as in the following form

$$\chi_{BAO}^2 = \frac{(\mathcal{A} - 0.469)^2}{0.017^2} \quad (30)$$

where the value of the parameter \mathcal{A} for the flat model ($k = 0$) of the FRW universe is obtained by $\mathcal{A} = 0.469 \pm 0.017$ using SDSS data set Eisenstein et al (2005) from luminous red galaxies survey. Now the total joint data analysis (Stern+BAO) for the χ^2 function defined by

$$\chi_{Tot}^2 = \chi_{Stern}^2 + \chi_{BAO}^2 \quad (31)$$

Now our best fit analysis with Stern+BAO observational data support the theoretical range of the parameters. In figures 6-8, we plot the graphs of (B_0, ω) for different confidence levels 66% (solid, blue), 90% (dashed, red) and 99% (dashed, black) contours for 4D, 5D and 6D respectively and by fixing the other parameters $\mu_0 = 0.7, \delta = 0.01, w_m = 0.1$. The best fit values of (B_0, ω) and minimum values of χ^2 for different values of $n = 2, 3, 4$ (i.e., different dimensions) are tabulated in table 3.

n	B_0	ω	χ_{min}^2
2(4D)	0.007	0.068	790.463
3(5D)	0.005	0.127	777.620
4(6D)	0.002	0.194	595.719

Table 3: $H(z)$ - z (Stern)+BAO: The best fit values of B_0 , ω and the minimum values of χ^2 for different dimensions.

4.3. Current Supernovae Type Ia Data

In this section, we use Supernova Type Ia data at high redshifts Perlmutter et al (1998, 1999); Riess et al (1998, 2004) and Baryonic Acoustic Oscillation (BAO) Eisenstein et al (2005) to restrict the parameters of the model for different dimensions. The observations directly measure the distance modulus of a Supernovae and its redshift z Riess et al; Kowalaski et al (2008). Now, take recent observational data, including SNe Ia which consists of 557 data points and belongs to the Union2 sample Amanullah et al (2010).

From the observations, the luminosity distance $d_L(z)$ determines the dark energy density and is defined by

$$d_L(z) = (1+z)H_0 \int_0^z \frac{dz'}{H(z')} \quad (32)$$

and the distance modulus (distance between absolute and apparent luminosity of a distance object) for Supernovas is given by

$$\mu(z) = 5 \log_{10} \left[\frac{d_L(z)/H_0}{1 \text{ Mpc}} \right] + 25 \quad (33)$$

The best fit of distance modulus as a function $\mu(z)$ of redshift z for our theoretical model and the Supernova Type Ia Union2 sample are drawn for different dimensions (4D,

5D and 6D) in figure 9 for our best fit values of ω and B_0 by fixing the other parameters $\mu_0 = 0.7, \delta = 0.01, w_m = 0.1$.

5. Discussions

In this work, we have considered the flat FRW model of the universe in $(n + 2)$ -dimensions filled with the dark matter and the magnetic field. We present the Hubble parameter in terms of the observable parameters Ω_{m0} and H_0 with the redshift z and the other parameters like $B_0, \omega, \mu_0, \delta, n, w_m$. The magnetic field B and deceleration parameter q have been calculated. The magnetic field B follows the power law form of redshift z . Now the variation of deceleration parameter q against redshift z has been plotted in figure 1 for 4D ($n = 2$), 5D ($n = 3$) and 6D ($n = 3$). From figure, we see that q decreases from some positive value to -1 as z decreases. So the model generates first deceleration and then acceleration as universe expands. Recently proposed Om diagnostic has also been discussed for our model. We draw the Om diagnostic against redshift z in figure 2 for 4D, 5D and 6D. The Om diagnostic always increases as z decreases (universe expands).

We have investigated the observational constraints of the higher dimensional FRW model of the magnetic universe. Here we have chosen the observed values of $\Omega_{m0} = 0.28, \Omega_{x0} = 0.72$ and $H_0 = 72 \text{ Kms}^{-1} \text{ Mpc}^{-1}$. From Stern data set (12 points), we have obtained the bounds of the arbitrary parameters by minimizing the χ^2 test. The best-fit values of the parameters are obtained by 66%, 90% and 99% confidence levels. Now to find the bounds of of the parameters (B_0, ω) and to draw the statistical confidence contour, we fixed four parameters $\mu_0 = 0.7, \delta = 0.01, w_m = 0.1$ and $n = 2, 3, 4$. Here the parameter n determines the higher dimensions and we perform comparative study between three cases : 4D ($n = 2$), 5D ($n = 3$) and 6D ($n = 4$) respectively. We have plotted the graphs for different confidence levels i.e., 66%, 90% and 99% confidence levels and for three different dimensions (4D, 5D and 6D) in figures 3-5. Now our best fit analysis with Stern observational data support the theoretical

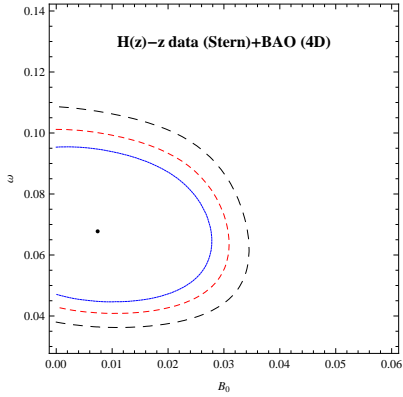


Fig.6

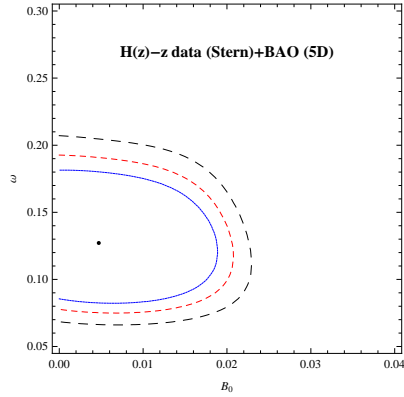


Fig.7

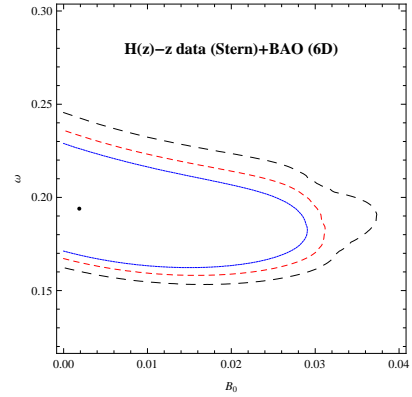


Fig.8

Figs. 6 - 8 show that the variations of ω against B_0 in 4D, 5D and 6D respectively for different confidence levels. The 66% (solid, blue), 90% (dashed, red) and 99% (dashed, black) contours are plotted in these figures for the $H(z)$ - z (Stern)+BAO joint analysis.

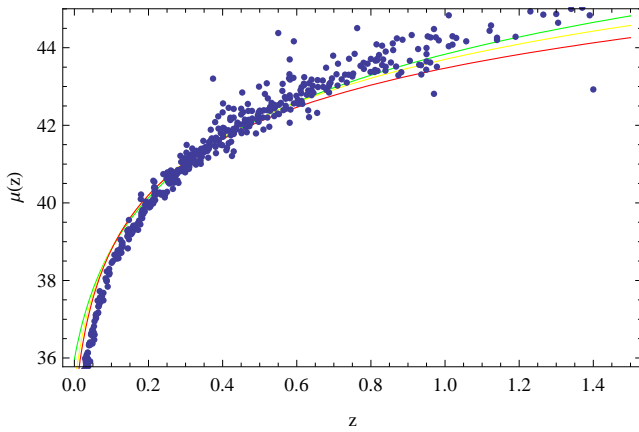


Fig.9

In fig.9, $\mu(z)$ vs z is plotted for our model (solid line) (green for 4D, yellow for 5D and red for 6D) and the Union2 sample (dotted points).

range of the parameters. The best fit values of (B_0, ω) and minimum values of χ^2 for different dimensions are tabulated in Table 2. For each dimension, we compare the model parameters through the values of the parameters and by the statistical contours. From this comparative study, one can understand the convergence of theoretical values of the parameters to the values of the parameters obtained from the observational data set and how it changes from normal four dimension to higher dimension (6D). Next due to joint analysis with Stern+BAO observational data, we have also obtained the bounds of the parameters (B_0, ω) by fixing some other parameters $\mu_0 = 0.7, \delta = 0.01, w_m = 0.1$ for 4D, 5D and 6D. In figures 6-8, we have plotted the graphs of (B_0, ω) for different confidence levels 66% (solid, blue), 90% (dashed, red) and 99% (dashed, black) contours for 4D, 5D and 6D respectively. The best fit values of (B_0, ω) and minimum values of χ^2 for different dimensions are tabulated in Table 3. The best fit of distance modulus as a function $\mu(z)$ of redshift z for our theoretical model and the Supernova Type Ia Union2 sample are drawn for different dimensions (4D, 5D and 6D) in figure 9 for our best fit values of ω and B_0 by fixing the other parameters $\mu_0 = 0.7, \delta = 0.01, w_m = 0.1$.

Acknowledgement:

The authors are thankful to IUCAA, Pune, India for warm hospitality where part of the work was carried out. Also UD is thankful to CSIR, Govt. of India for providing research project grant (No. 03(1206)/12/EMR-II).

REFERENCES

- Amanullah, R., et al. *Astrophys. J.*, **716**, 712(2010).
- Anninos, D. and Pastras, G. *J. High. Energy Phys.*, **07**:030(2009).
- Armendariz - Picon, C., Mukhanov, V. F. and Steinhardt, P. J., *Phys. Rev. D*, **63**:103510(2001).
- Ashtekar, A., et al., *Class. Quant. Grav.*, **28**:213001(2011).
- Ayn-Beato, E. and Garca, A. *Phys. Rev. Lett.*, **80**:5056(1998).
- Ayn-Beato, E. and Garca, A. *Phys. Lett. B*, **464**:25(1999).
- Bachall, N. A., et al., *Science*, **284**:1481(1999).
- Balart, L., et al., *Eur.Phys.J. C*, **51**:185(2007).
- Bandyopadhyay, T. and Debnath, U., *Phys. Lett. B*, **704**:95(2011).
- Bennet, C., et al., *Phys. Rev. Lett.*, **85**:2236(2000).
- Born, M. and Infeld, L. *Proc. R. Soc. A*, **144**:425(1934).
- Bouhmadi-Lpez, M. and Chimento, L. P., *Phys.Rev. D*, **82**:103506(2010).
- Brans, C. and Dicke, R.H., *Phys. Rev.*, **124**:925(1961).
- Bridle, S., et al., *Science*, **299**:1532(2003).
- Bronnikov, K. A., et al., *Phys. Rev. D*, **86**:024028(2012)
- Cai, R. G., et al., *Phys. Rev. D*, **78**:126007(2008).
- Caldwell, R.R., *Phys. Lett. B*, **545**:23(2002).
- Camara, C. S., et al., *Phys. Rev. D*, **69**:123504(2004).
- Chakraborty, S. and Debnath, U., *Int. J. Theor. Phys.*, **24**:25(2010).
- Chakraborty, S., Debnath, U. and Ranjit, C., *Eur. Phys. J. C*, **72**, 2101(2012).

- Chang, H. Y. and Scherrer, R. J., *Phys. Rev. D*, **86**:027303(2012)
- Chatterjee, S., arXiv:0911.2621 [gr-qc].
- Cognola, G., et al., *Phys. Rev. D*, **79**:044001(2009).
- De Lorenci, V. A., Klippert, R., Novello, M. and Salim, J. M. *Phys. Rev. D*, **65**:063501(2002).
- De Sitter, W., *Proc. K. Ned. Akad. Wet.*, **19**:1217(1917).
- Del Campo, S., Herrera, R. and Toloza, A., *Phys.Rev.D*, **79**:083507(2009).
- Eisenstein, D. J., et al. *Astrophys. J.*, **633**, 560(2005).
- Farajollahi, H. and Ravanpak, A., *Phys.Rev.D*, **84**:084017(2011).
- Garca-Salcedo, R. and Breton, N. *IJMPA*, **15**:4341(2000).
- Garca-Salcedo, R. and Breton, N. *Class. Quant. Grav.*, **22**:4783(2005).
- Gergely, L. A. and Maartens, R., *Class. Quant. Grav.*, **19**:213(2002)
- Ghose, S., Thakur, P. and Paul, B. C. *arXiv: 1105.3303v1* [astro-ph.CO].
- Heisenberg, W. and Euler, H. *Z. Phys.*, **98**:714(1936).
- Kats, Y., et al., *J. High. Energy Phys.*, **12**:068(2007).
- Klippert, R., De Lorenci, V. A., Novello, M. and Salim, J. M. *Phys. Lett. B*, **472**:27(2000).
- Kolb, E. W. and Turner, M. S. *The Early Universe*, Addison-Wesley, Redwood City, CA (1990).
- Kowalaski et al. *Astrophys. J.*, **686**, 749(2008).
- Lu, J., et al. *Int. J. Mod. Phys. D*, **18**:1741(2009).
- Malquarti, M., et al., *Phys. Rev. D*, **68**: 023512(2003).
- Marcus, N., *Gen. Rel. Grav.*, **22**:873(1990).

- Martin, J. and Yamaguchi, M., *Phys. Rev. D*, **77**:123508(2008).
- Miller, D., et al., *Astrophys. J.*, **524**:L1(1999).
- Morris, J. R., *Gen. Rel. Grav.*, **44**:437(2012).
- Mukhopadhyay, U., Ghosh, P. P. and Ray, S., arXiv:1001.0475[gr-qc].
- Munõz, G. *Am. J. Phys.*, **64**:1285(1996).
- Murphy, G. L., *Phys. Rev. D*, **8**:4231(1973).
- Novello, M. and Salim, J. M. *Phys. Rev. D*, **20**:377(1979).
- Novello, M., et al., *IJMPA* **1**:641(1993).
- Novello, M., Oliveira, L. A. R. and Salim, J. M. *Class.Quantum Grav.*, **13**:1089(1996).
- Novello, M., Bergliaffa, S. E. P. and Salim, J., *Phys. Rev. D* **69** 127301 (2004).
- Novello, M. *Int. J. Mod. Phys. A*, **20**:2421(2005).
- Padmanabhan, T., *Phys. Rept.*, **380**:235(2003).
- Paul, B. C., Ghose, S. and Thakur, P., *arXiv: 1101.1360v1* [astro-ph.CO].
- Paul, B. C., Thakur, P. and Ghose, S., *arXiv: 1004.4256v1* [astro-ph.CO].
- Peebles, P. J. E. and Ratra, B., *Astrophys. J. Lett.*, **325**:L17(1988).
- Perlmutter, S. J., et al., *Nature*, **391**:51(1998).
- Perlmutter, S. J., et al., *Astrophys. J.*, **517**:565(1999).
- Ranjit, C., et al., *Int. J. Theor. Phys.*, **51**:2180(2012).
- Riess, A. G., et al., *Astron. J.*, **116**:1009(1998).
- Riess, A. G., et al., *Astrophys. J.*, **607**:665(2004).
- Riess, A. G., et al. *Astrophys. J.*, **659**, 98(2007).

Sahni, V. and Starobinsky, A. A., *Int. J. Mod. Phys. D*, **9**:373(2000).

Sahni, V., et al., *JETP Lett.*, **77**:201(2003).

Sahni, V., et al., *Phys. Rev. D*, **78**:103502(2008).

Salazar, H., et al., *J. Math. Phys.*, **28**:2171(1987).

Schwinger, J. *Phys. Rev.*, **82**:664(1951).

Sen, A., *JHEP*, **0207**:065(2002).

Spalinski, M., *J. Cosmol. Astropart. Phys*, **05**:017(2007).

Spergel, D. N., et al., *Astrophys. J. Suppl.*, **148**:175(2003).

Stern, D., et al. *JCAP*, **1002**, 008(2010).

Tedmark, M., et al., *Phys. Rev. D*, **69**:103501(2004).

Thakur, P., Ghose, S. and Paul, B. C., *Mon. Not. R. Astron. Soc.*, **397**, 1935(2009).

Tong, M. L. and Zhang, Y., *Phys. Rev. D*, **80**:023503(2009).

Wei, H., et al., *Class. Quantum. Grav.*, **22**:3189(2005).

Wu, P., and Yu, H., *Phys. Lett. B*, **644**, 16(2007).